European Journal of Medicinal Chemistry 203 (2020) 112540

Contents lists available at ScienceDirect

European Journal of Medicinal Chemistry

journal homepage: http://www.elsevier.com/locate/ejmech

Research paper

Fluoropyrimidin-2,4-dihydroxy-5-isopropylbenzamides as antitumor agents against CRC and NSCLC cancer cells

Wei-Cheng Wu [a, 1], Yi-Min Liu [a, b, f, 1], Yu-Hsuan Liao [d], Kai-Cheng Hsu [b, e], Ssu-Ting Lien [e], I-Chung Chen [a], Mei-Jung Lai [b], Yu-Hsuan Li [a], Shiow-Lin Pan [a, b, e], Mei-Chuan Chen [a, c, d, *], Jing-Ping Liou [a, b, **]

[a] School of Pharmacy, College of Pharmacy, Taipei Medical University, Taiwan
[b] TMU Biomedical Commercialization Center, Taipei Medical University, Taiwan
[c] Traditional Herbal Medicine Research Center of Taipei Medical University Hospital, Taipei, Taiwan
[d] Ph.D. Program in Clinical Drug Development of Herbal Medicine, College of Pharmacy, Taipei Medical University, Taiwan
[e] Graduate Institute of Cancer Biology and Drug Discovery, College of Medical Science and Technology, Taipei Medical University, Taipei, Taiwan
[f] Faculty of Pharmaceutical Sciences, Hokkaido University, Sapporo, Japan

ARTICLE INFO

Article history:
Received 28 February 2020
Received in revised form
26 May 2020
Accepted 4 June 2020
Available online 16 July 2020

Keywords:
Non-small cell lung cancer (NSCLC)
Colorectal cancer (CRC)
HSP90 inhibitors

ABSTRACT

A major cause of failure of therapy in patients with non-small cell lung cancer (NSCLC) is development of acquired drug resistance leading to tumor recurrence and disease progression. In addition to the development of new generations of epidermal growth factor receptor-tyrosine kinase inhibitors (EGFR-TKIs), different molecular targets may provide opportunities to improve the therapeutic outcomes. In this study, we utilized the core structure 5-fluorouracil (5-FU) or tegafur, a 5-FU prodrug combined through different linkers with resorcinol to generate a series of fluoropyrimidin-2,4-dihydroxy-5-isopropylbenzamides which inhibit potent Heat Shock Protein 90 (HSP90). These compounds were found to show significant antiproliferative activity in colorectal cancer (CRC) HCT116 and NSCLC A549, H460, and H1975 (EGFR L858R/T790 M double mutation) cells. Compound **12c**, developed by molecular docking analysis and enzymatic assays exhibits promising inhibitory activity of HSP90. This compound, **12c** shows the most potent HSP90 inhibitory activity with an IC_{50} value of 27.8 ± 4.4 nM, superior to that of reference compounds AUY-922 (Luminespib) and BIIB021 whose IC_{50} values are 43.0 ± 0.9 nM and 56.8 ± 4.0 nM respectively. This strong HSP90 inhibitory activity of **12c** leads to rapid degradation of client proteins EGFR and Akt in NSCLC cells. In addition, **12c** induces significant accumulation of a sub-G1 phase population in parallel with apoptosis by showing activated caspase-3, -8 and -9 and PARP induction. These results provide a new strategy for development of novel HSP90 inhibitors for cancer treatment.

1. Introduction

Heat shock proteins (HSP) function as molecular chaperones that are responsible for proper folding, assembly, translocation, and degradation of proteins during essential cellular growth and development [1]. HSPs are widely expressed in plants and animals and are classified into different families based on their molecular weight [2]. Among HSP families, the role of HSP90 is the most characterized and well-studied. HSP90 is physically associated with numerous co-chaperones such as HSP70, to recruit and interact with diverse substrate or client proteins such as kinases, leading to regulation of cellular processes [3]. In addition, HSP90 has been widely reported to be involved in many human diseases, including neurodegenerative diseases, senescence, cancer and infectious diseases [4]. A number of HSP90 client proteins such as Akt, focal adhesion kinase (FAK) and transcription factor hypoxia-inducible factor 1α (HIF1α) are involved in tumor proliferation and metastasis [5]. Increased expression of HSP90 is easily detected in many malignancies and is associated with poor prognosis [6]. Consequently, targeting of HSP90 can be effective for cancer treatment

*Corresponding author. Ph.D. Program in Clinical Drug Development of Herbal Medicine, College of Pharmacy, Taipei Medical University, Taiwan.
** Corresponding author. School of Pharmacy, College of Pharmacy, Taipei Medical University, Taiwan.
E-mail addresses: mcchen1250@tmu.edu.tw (M.-C. Chen), jpl@tmu.edu.tw (J.-P. Liou).
[1] Contributed equally to this work.

https://doi.org/10.1016/j.ejmech.2020.112540
0223-5234/

since HSP90 inhibition will result in interruption of many crucial signaling pathways that are crucial to cancer cell survival. Several HSP90 inhibitors have been developed and are divided into different subgroups based on their structures. For example, resorcinol-based HSP90 inhibitors can be found in a number of clinical trials subjects such as AUY-922 (**1**, Luminespib), STA-9090 (**2**, Ganetespib) and AT-13387 (**3**, Onalespib) (Fig. 1) [7]. These resorcinol-containing compounds have been reported to be active against NSCLC, CRC and other different types of tumors [8].

5-Fluorouracil (**4,** 5-FU), an analogue of uracil (**5**) with a fluorine atom at the C-5 position, is converted to several active metabolites to further replace the normal uracil and interrupt the nucleotide synthesis which results in DNA damage in cancer cells [9]. Currently, FOLFIRI a combination of folinic acid (**8**), 5-FU and irinotecan (**6**) and FOLFOX (folinic acid, fluorouracil, oxaliplatin (**7**)) are approved for clinical CRC regimens [10]. Tegafur (**9**) and capecitabine (**10**) are prodrugs of 5-FU which are converted intracellularly to active metabolites leading to potent cytotoxicity [11]. Previous reports have suggested that combination therapy of standard regimen FOLFIRI with cetuximab or bevacizumab may improve outcomes in patients with metastatic colorectal cancer [12] and several studies have shown that administration to NSCLC patients of tegafur or capecitabine in combination with other drugs helps to increase patient survival rates [13]. These results suggest one-compound-multi-target agents could be effective and they represent a promising strategy for CRC and NSCLC treatment.

The major clinical challenge in treatment of NSCLC is the development of acquired resistance to drugs [14]. The best study of acquired resistance to epidermal growth factor receptor (EGFR)-TKI is a secondary mutation (T790 M) in exon 20 of EGFR in patients with NSCLC [15]. In order to overcome the resistance to EGFR-TKIs, different types of TKIs and other molecular targeted therapies have been developed with a view to extending disease control [16]. MET amplification, overexpression of hepatocyte growth factor (HGF) and activation of the insulin-like growth factor 1 receptor (IGF1R) have been identified as crucial mechanisms underlying acquired

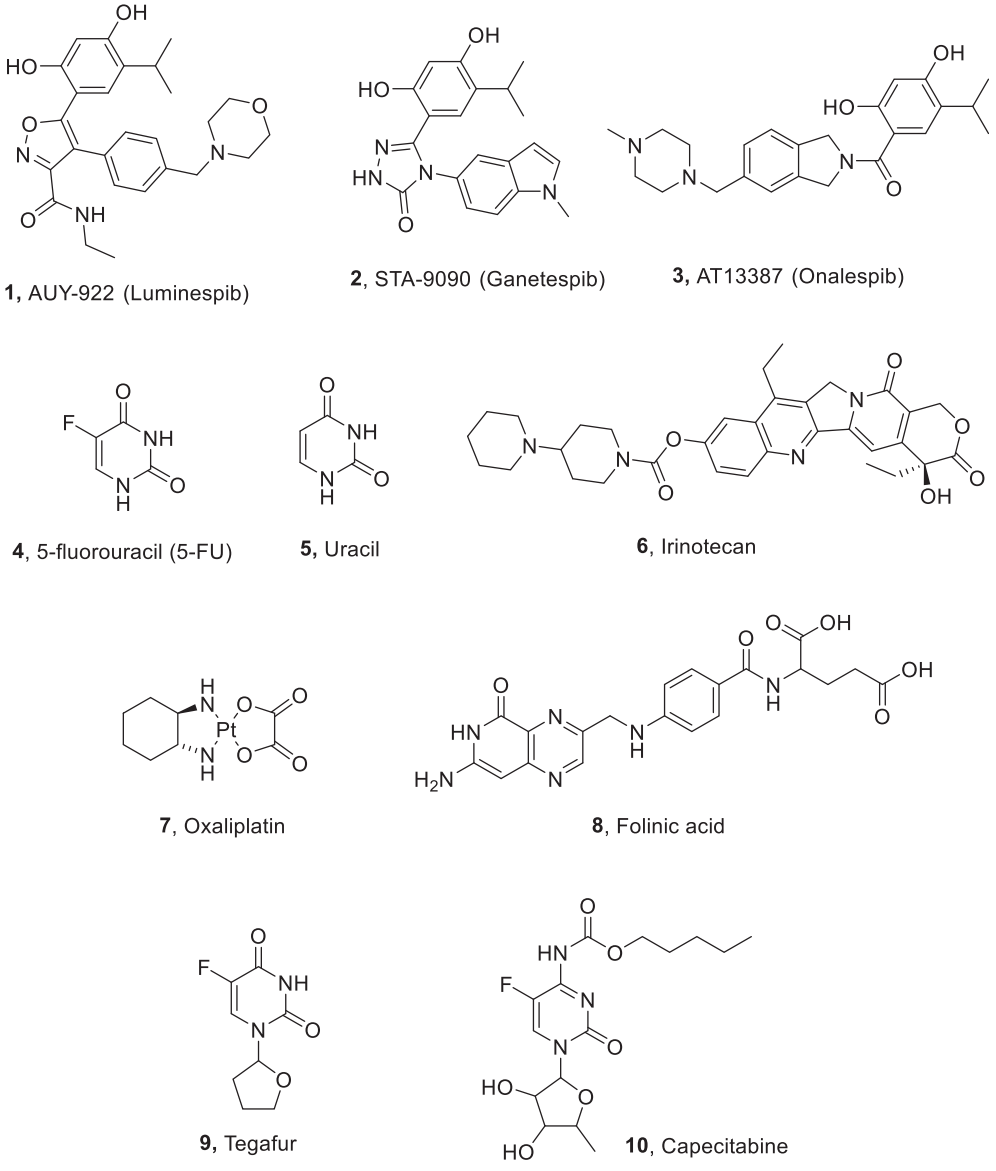

Fig. 1. Reported chemotherapeutic agents and HSP90 inhibitors.

resistance to EGFR-TKIs [17]. Previous reports also indicate that EGFR-TKIs, in combination with other targeted drugs such as VEGF, MEK/ERK or HER2 have shown some potential ability to overcome resistance mediated by different mechanisms [18].

Based on previous studies, inhibitors of 5-FU and HSP90 have shown some success in patients with NSCLC [19]. Therefore, we combined the structure of tegafur or 5-FU with resorcinol to exert cytotoxic and HSP90 inhibitory activity and so decrease oncogenic client proteins and enhance the anticancer activity for NSCLC therapy (Fig. 2). A series of compounds (**12**–**13**) was synthesized (Fig. 3) and their biological assays are discussed below.

2. Results and discussion

2.1. Chemistry

Tagafur (**6**) reacted with 4-nitrobenzyl bromide in the presence of K_2CO_3, yielding compound **14** (Scheme 1). Compound **14** with a nitro group was reduced with iron powder and ammonium chloride in isopropanol and water to afford the amino compound **(15)**. Compound **15** underwent amide coupling with 1-ethyl-3-(3-dimethylaminopropyl)carbodiimide hydrochloride (EDC·HCl), 1-hydroxybenzotriazole (HOBt), N-methylmorpholine (NMM) and 2,4-bis(benzyloxy)-5-isopropylbenzoic acid to produce compound **16**. The protected compound (**16**) was debenzylated by Pd/C and hydrogen affording compound **12a**. Compounds **12b-12h** and compounds **13a-13c** were prepared similarly from compound **16** and various substituted groups under basic conditions. The deprotection can be accomplished with hydrogen gas and palladium or with boron trichloride, as is shown in Scheme 2.

2.2. Biological evaluation

2.2.1. HSP90 inhibition

We first evaluated the HSP90 inhibitory activity of synthetic compounds **12a-12h** and **13a-13c** together with reference compounds AUY-922 and BIIB021, as shown in Table 1. Compound **12a**, lacking substitution at the amide linkage, showed no HSP90 inhibitory activity. However, compounds **12b-12h** and **13a-13c** with the N-substituted groups displayed good inhibitory activity against HSP90. Most of synthetic compounds have IC_{50} values against HSP90 of ~50 nM which is comparable to those of the reference compounds. Compound **12c** with an ethyl group showed the strongest HSP90 inhibitory activity, suggesting the activity is related to the length of substituent group. The N-substituted benzyl group compounds **12f-12h**, and **13a-13c**, also displayed significant activity and showed inhibitory activity comparable to that of the reference compounds. Among the synthesized compounds, compound **12c** exhibited remarkable HSP90 inhibitory activity with an $IC_{50} = 27.8$ nM, which is about two-fold stronger than the reference compounds.

2.2.2. In vitro cell growth inhibitory activity

In an attempt to evaluate the effect of the synthetic compounds on growth inhibition of cancer cells, we examined synthesized compounds **12a-12h** and **13a-13c** for anti-proliferative activity against CRC HCT116 cells (Table 2). Compared to compound **4** (5-FU), most of synthesized compounds displayed potent inhibitory activities in CRC cells. In addition, the observed pattern of inhibitory activity is consistent with the HSP90 inhibition shown in Table 1. Compound **12c** exhibited anticancer activity with a GI_{50} value of 10 ± 1 nM which is 15 times more inhibitory than reference

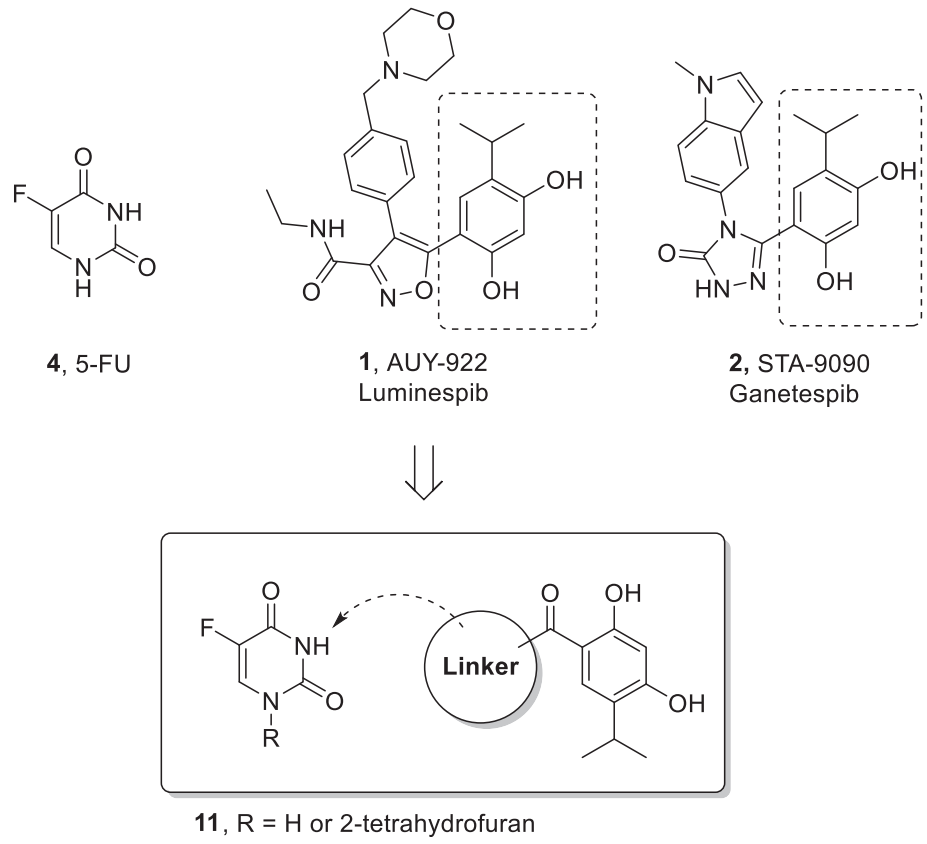

Fig. 2. Rational design of target compounds.

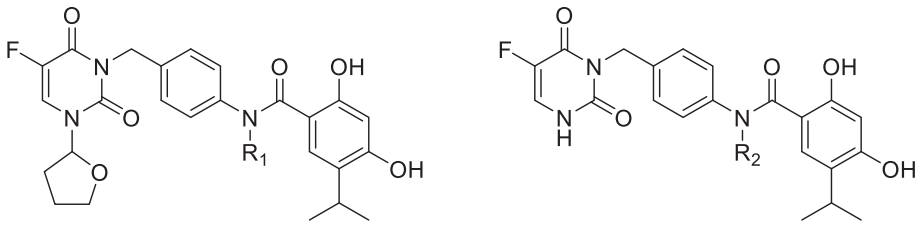

12a, R_1 = H
12b, R_1 = methyl
12c, R_1 = ethyl
12d, R_1 = propyl
12e, R_1 = benzyl
12f, R_1 = 4-cyanobenzyl
12g, R_1 = 4-chlorobenzyl
12h, R_1 = 4-methoxybenzyl

13a, R_2 = ethyl
13b, R_2 = $CH_2CH{=}CH_2$
13c, R_2 = $CH_2C{\equiv}CH$

Fig. 3. Structures of synthetic compounds (**12**–**13**).

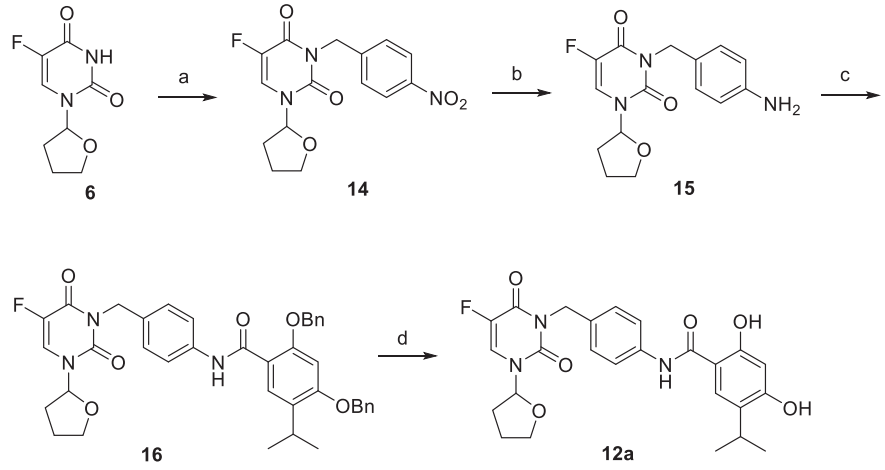

[a]Reagents and condition: (a) 4-nitrobenzyl bromide, K_2CO_3, DMF, rt; (b) Iron powder, NH_4Cl, IPA/H_2O, reflux; (c) EDC·HCl, HOBt, NMM, 2,4-bis(benzyloxy)-5-isopropylbenzoic acid , DMF, rt; (d) H_2, 10% Pd/C, MeOH, rt

Scheme 1. Synthetic route of compound **12a**[aa]Reagents and condition: (a) 4-nitrobenzyl bromide, K_2CO_3, DMF, rt; (b) Iron powder, NH_4Cl, IPA/H_2O, reflux; (c) EDC·HCl, HOBt, NMM, 2,4-bis(benzyloxy)-5-isopropylbenzoic acid, DMF, rt; (d) H_2, 10% Pd/C, MeOH, rt.

compound BIIB021.

2.2.3. *In vitro cell growth inhibitory activity against human lung cancer cell lines*

It has been reported that HSP90 inhibitors such as STA-9090 and AUY-922 display good activity against lung cancer cells [20]. Therefore we also investigated the effect of synthetic compounds against various human lung cancer cell lines, including two carrying wild-type EGFR (A549 and H460), and one EGFR L858R/T790 M double mutations (H1975). As shown in Table 3, a majority of our synthetic compounds have shown the ability to suppress cell proliferation in these three human NSCLC cells independently of their EGFR status. Compounds **13a**-**13c** exhibit more potent cell growth inhibitory activity than compounds **12b**-**12h**, suggesting that 5-FU plus resorcinol generates higher cytotoxicity *in vitro* than tegafur-resorcinol. It is surprising that the H1975 cell line is the most sensitive to many of the compounds among **12c**-**12h**, suggesting that if R_1 is benzyl, cyanobenzyl or chlorobenzyl the compound may provide some selectivity toward H1975 cells with the EGFR L858R/T790 M double mutation. Compound **12c**, with the best activity against CRC HCT116 cells, as shown in Table 2, also demonstrated promising antiproliferative activity with GI_{50} values of 0.07, 0.06, and 0.04 μM against A549, H460 and H1975 NSCLC cells, respectively.

2.2.4. *Colony formation in evaluation of antitumor activity in different cancer cells*

We examined the colony forming ability of compound **12c** in cells of three different cancers. Although compound **12c** exhibits better antiproliferative activity in CRC HCT116 cells than other tumor cells (Tables 2 and 3), the colony-forming results showed a better inhibitory effect toward NSCLC A549 and H1975 cells with the same concentrations (0.009 μM and 0.018 μM) of **12c** (Fig. 4A–C). Taken together, these results show compound **12c** caused a significant inhibition of cell growth and colony-forming ability in NSCLC cells, suggesting **12c** may provide potentially

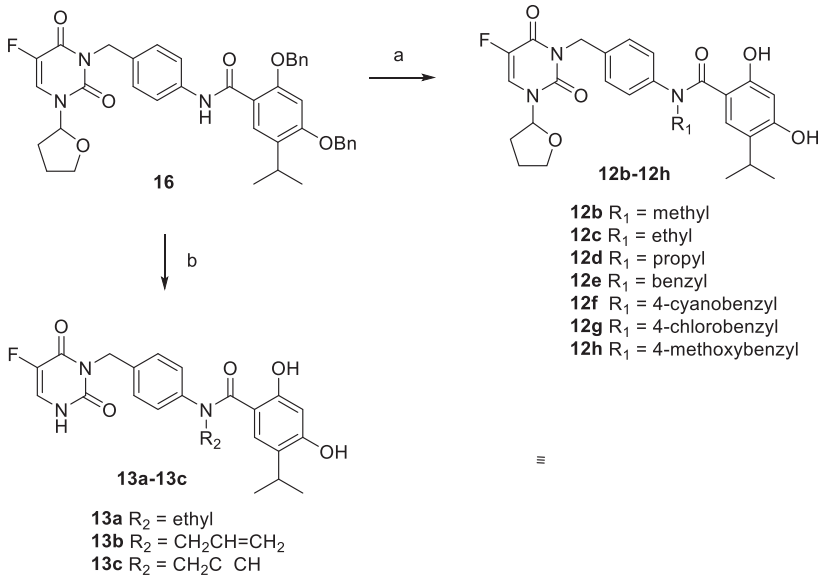

[a]Reagents and condition: (a) i. NaH, various substituted group, DMF, rt; ii. H_2, 10% Pd/C, MeOH, rt, (b) i. NaH, various substituted group, DMF, rt; ii. BCl_3, CH_2Cl_2, 0°C to rt

Scheme 2. Synthetic route of compounds **12b-12h** and **13a-13c**[a].
[a]Reagents and condition: (a) i. NaH, various substituted group, DMF, rt; ii. H_2, 10% Pd/C, MeOH, rt, (b) i. NaH, various substituted group, DMF, rt; ii. BCl_3, CH_2Cl_2, 0 °C to rt.

Table 1
HSP90α inhibition of synthetic compounds (**12a-12h** and **13a-13c**) and reference compounds.

Compounds	HSP90α IC_{50}(nM ± SD[a])	Compounds	HSP90α IC_{50}(nM ± SD[a])
12a	>1000	**12h**	58.8 ± 6.9
12b	40.9 ± 19.3	**13a**	44.9 ± 0.8
12c	27.8 ± 4.4	**13b**	48.0 ± 1.5
12d	48.2 ± 13.8	**13c**	54.4 ± 0.6
12e	45.3 ± 5.0	AUY-922 (**1**)	43.0 ± 0.9
12f	45.3 ± 7.0	BIIB021	56.8 ± 4.0
12g	54.7 ± 16.3		

[a] SD: standard deviation. All experiments were independently performed at least three times.

useful antitumor activity for NSCLC treatment.

2.2.5. Evaluation of expression level of Hsp90 client proteins

Next, we examined some critical biomarkers of Hsp90 inhibition in A549 and H1975 cells. Inhibition of HSP90 will lead to heat shock factor 1 (HSF1) activation, consequently inducing several small heat shock proteins to help appropriate folding of misfolded proteins [21]. As shown in Fig. 5A and B, treatment with compound **12c** greatly induced the expression level of HSP70 without affecting HSP90 levels. Furthermore, several client proteins such as protein kinase B (akt) and EGFR were also downregulated in response to compound **12c**, indicating compound **12c** achieves significant suppression of HSP90 activity in cells.

2.2.6. Evaluation of cell cycle progression and cell death response

We examined the effects of compound **12c** on cell cycle progression using flow cytometry. Notably, the subG1 phase showed a dramatic induction after 48 h of treatment (Fig. 6A and B) in parallel with significant activation of caspase-3, -8, and -9, and poly-(ADP-ribose) polymerase (PARP) (Fig. 7A and B). These results suggest that compound **12c** induces significant apoptotic cell death in NSCLC.

2.2.7. Molecular docking study

Molecular docking analysis was performed to illuminate the interactions between **12c** and HSP90 (PDB ID: 5GGZ). The docking pose of **12c** in HSP90, can be separated into four distinct sites (Fig. 8). In Site 1 (S1), the resorcinol group of **12c** forms hydrogen bonds with residues Leu48, Asp93, and Thr184, and hydrophobic interactions occur between its isopropyl moiety and residues Leu48 and Phe138, while the benzene ring creates hydrophobic interactions with residues Ala55 and Val186. Site 2 (S2) contains an

Table 2
Antiproliferative activity (GI_{50}) of synthetic compounds (**12a-12h** and **13a-13c**) against colorectal HCT116 cancer cell line.

Compounds	HCT116 GI_{50} (μM ± SD[a])	Compounds	HCT116 GI_{50} (μM± SD[a])
12a	>10	**13a**	0.030 ± 0.001
12b	0.120 ± 0.010	**13b**	0.080 ± 0.001
12c	0.010 ± 0.001	**13c**	0.040 ± 0.006
12d	0.960 ± 0.210	STA-9090 (**2**)	0.150 ± 0.020
12e	0.780 ± 0.002	5-FU (**4**)	>10
12f	0.410 ± 0.050	Tegafur (**9**)	>10
12g	0.700 ± 0.110	BIIB021	0.150 ± 0.020
12h	0.720 ± 0.011		

[a] SD: standard deviation. All experiments were independently performed at least three times.

Table 3
Antiproliferative activity (GI_{50}) of compounds (**12a-12h** and **13a-13c**) against lung A549, H460 and H1975 cancer cell line.

Compounds	A549 GI_{50} (μM ± SD[a])	H460 GI_{50} (μM ± SD[a])	H1975 GI_{50} (μM ± SD[a])
12a	>10	>10	>10
12b	0.09 ± 0.01	0.07 ± 0.03	0.06 ± 0.00
12c	0.07 ± 0.01	0.06 ± 0.01	0.04 ± 0.00
12d	0.65 ± 0.03	0.52 ± 0.12	0.34 ± 0.03
12e	0.80 ± 0.07	0.40 ± 0.19	0.16 ± 0.04
12f	0.35 ± 0.04	0.20 ± 0.08	0.13 ± 0.01
12g	0.56 ± 0.03	0.46 ± 0.08	0.16 ± 0.03
12h	0.92 ± 0.11	0.39 ± 0.16	0.23 ± 0.05
13a	0.04 ± 0.00	0.03 ± 0.01	0.03 ± 0.00
13b	0.10 ± 0.01	0.07 ± 0.01	0.05 ± 0.02
13c	0.03 ± 0.00	0.07 ± 0.02	0.02 ± 0.00
AUY922 (**1**)	0.01 ± 0.00	0.03 ± 0.01	0.02 ± 0.00
5-FU (**4**)	19.76 ± 2.9	–	–
Tegafur (**9**)	>50	–	–
BIIB021	0.26 ± 0.04	0.21 ± 0.10	0.20 ± 0.06

[a] SD: standard deviation. All experiments were independently performed at least three times.

N-ethyl moiety that occupies a hydrophobic pocket formed by residues Ala55, Met98 and Tyr61. The phenyl group at Site 3 (S3) occupies a cavity within the binding site and serves as a linker between the ethyl and the tegafur moiety at Site 4 (S4). The tegafur moiety forms hydrogen bonds with residues Asn51 and Phe138. When comparing **12c** with its derivatives, **12c** has an increased HSP90 inhibitory effect over that of its derivatives, such as unsubstituted **12a** and **12b** with a methyl group in place of the ethyl moiety. These differences reduce their inhibitory effect against HSP90 (Table 1). Consequently, it could be concluded that the ethyl moiety in **12c** is important for its activity against HSP90.

To further elucidate interactions between compound **12c** and HSP90, we compared the compound to the co-crystal ligand, 6 TN. We observed an overlap at Site 1 and Site 2 (Fig. 8C). This co-crystal ligand also contains a resorcinol group at Site 1. Hydrogen bonds form with residues Asp93 and Thr184 at Site 1. Residues Thr184 and Ala55 form hydrophobic interactions with the benzene ring. An isopropyl moiety is attached to the benzene ring and forms further hydrophobic interactions with residues Phe138 and Val150. The co-crystal ligand also contains a pyridopyrimidine structure. A part of this moiety occupies Site 2, forming hydrophobic interactions with residues Ala55, Met98 and Leu107. Because of its position, the co-crystal ligand does not align with Site 3 and Site 4. The reported IC_{50} value of co-crystal ligand is 56 nM [22]. When compared to compound **12c**, the difference in potency may be due to its interactions at Site 3 and Site 4.

We previously found that compound **12c** has a comparable IC_{50} value to the HSP90 inhibitor AUY-922 (Table 1). A co-crystal structure of HSP90 with AUY-922 has been determined previously (PDB ID: 2VCI) [23]. As a result, we compared compound **12c** to the AUY-922 co-crystal ligand. We found that both compounds align with the four distinct sites (Fig. 8D). AUY-922 also contains a resorcinol and isopropyl moiety that occupies Site 1, similar to compound **12c**. Hydrogen bonds are formed with residues Asn51, Asp93 and Thr184. The isopropyl moiety occupies a similar hydrophobic pocket by residues Leu107 and Phe138. At Site 2, residues Lys58 and Gly97 form hydrogen bonds to the oxygen and nitrogen of the N-ethylformamide, respectively. Further hydrophobic interactions by residue Ala55 occur at Site 3. However, Site 4 did not show stable interactions between AUY-922 and HSP90. The additional hydrogen bond at Site 3 and hydrophobic interactions at Site 4 suggests areas that can be exploited for HSP90 inhibition. Together, the molecular docking analysis is consistent with the potency of **12c** against HSP90.

3. Conclusion

In this study, a series of fluoropyrimidin-2,4-dihydroxy-5-isopropylbenzamides (**12**–**13**) were synthesized as HSP90 inhibitors in an attempt to explore the compounds' biological activity against CRC and NSCLC. Among all the synthesized compounds, compound **12c** displays remarkable activity with an IC_{50} value of 27.8 nM in inhibition of HSP90 activity. In *in vitro* cell growth inhibition, **12c** not only shows good activity against HCT116 cancer cell with a GI_{50} value of 0.01 μM but also exhibits good activity with GI_{50} values of 0.07, 0.06, and 0.04 μM against A549, H460 and H1975 human NSCLC cell lines, respectively. In addition, compound **12c** significantly reduces the client proteins EGFR and Akt and induces apoptotic cell death in NSCLC cells. In this study, we have developed **12c** as a potential agent and a new strategy for development of novel HSP90 inhibitors for the treatment of cancer.

4. Experimental section

4.1. Chemistry

Nuclear magnetic resonance (^1H and ^{13}C NMR) spectra were obtained with Bruker DRX-500 spectrometer operating at 500 and 125 MHz and Bruker Fourier 300 and 75 MHz. Chemical shifts are reported in parts per million (ppm, δ) downfield from TMS as an internal standard. High-resolution mass spectra (HRMS) were measured with AB SCIE X (QSTAR® XL) High Resolution Electrospray (ESI) Mass Spectrometry spectrometer. Melting points were measured with Buchi B-545 (Buchi, Switzerland). Purity of the final compounds was achieved with a Waters Acquity UPLC system using C-18 column (Waters Acquity UPLC BEH C18, 1.7 μm, 2.1 mm × 50 mm). Flash column chromatography used silica gel: SILICYCLE (SiliaFlash Irregular Silica Gel P60, 40–63 μm, 60 Å (R12030B).

4.1.1. *N-(4-((5-Fluoro-2,6-dioxo-3-(tetrahydrofuran-2-yl)-3,6-dihydropyrimidin-1(2H)-yl)methyl)phenyl)-2,4-dihydroxy-5-isopropylbenzamide* ***(12a)***

A mixture of **16** (2.05 mmol), 10% palladium on carbon (0.4 g) in MeOH (40 ml) was stirred at room temperature (rt) under hydrogen overnight. The organic layer was filtered and the residue was purified by flash chromatography over silica gel to afford compound **12a** in 46% yield. ^1H NMR (500Hz, DMSO-d_6) δ (ppm): 1.17 (d, J = 6.9Hz, 6H), 1.90–1.93 (m, 2H), 2.02–2.04 (m, 1H), 2.21–2.28 (m, 1H), 3.07–3.13 (m, 1H), 3.81 (q, J = 7.5Hz, 1H), 4.22–4.26 (m, 1H),

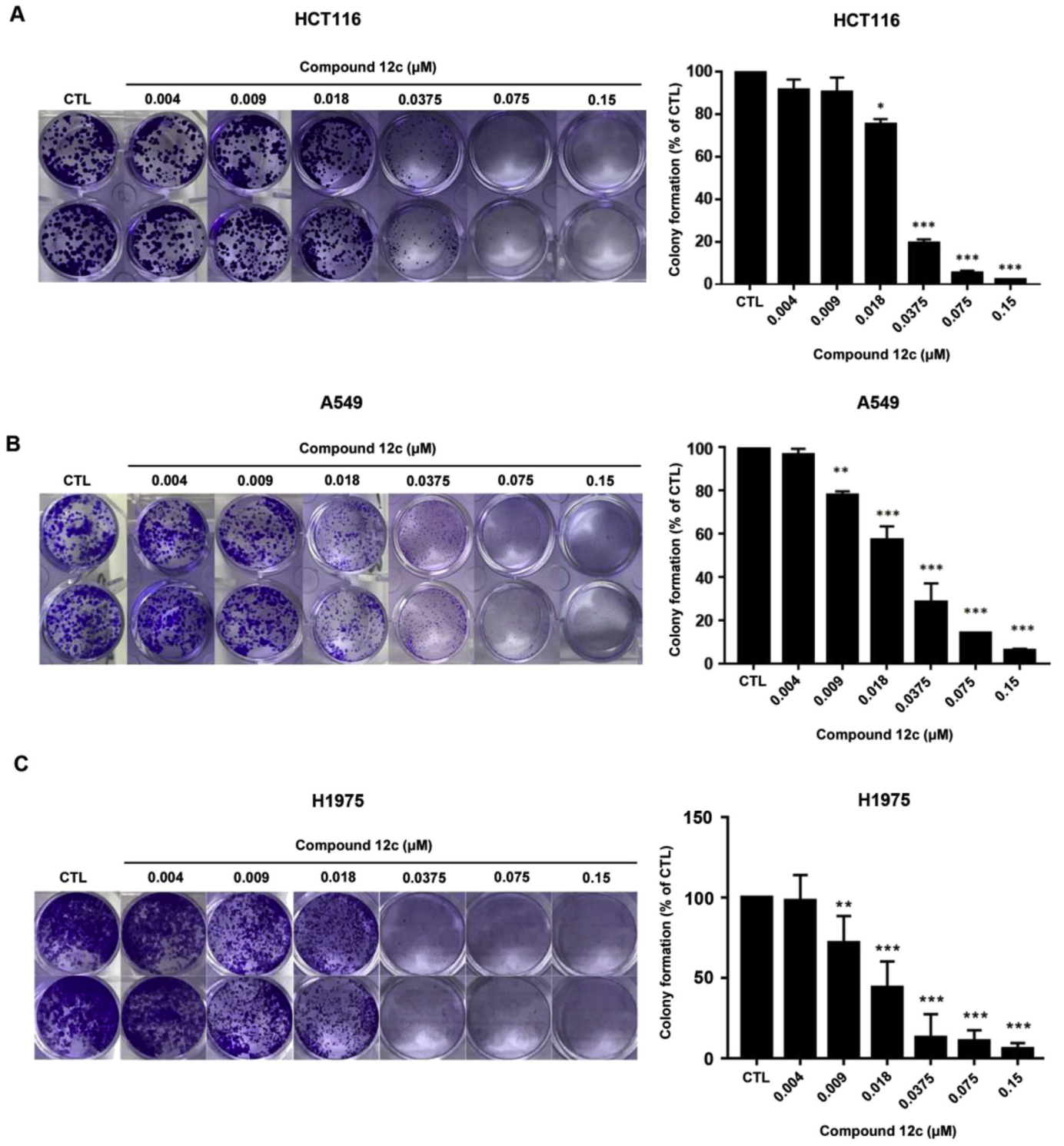

Fig. 4. Compound **12c** suppresses colony formation in colorectal (CRC) and non-small cell lung cancer (NSCLC) cells. (A–C) Compound **12c**-mediated concentration-dependent inhibition of colony formation in three different tumor cells lines (left panel) and quantification of colony numbers, expressed as a percentage of controls (right panel). Data are expressed as means ± S.D. of at least three independent experiments. *, $P < 0.05$; **, $P < 0.01$; and ***, $P < 0.001$ compared with the control group.

4.95 (d, J = 4.5Hz, 2H), 5.95–5.97 (m, 1H), 6.35 (s, 1H), 7.29 (d, J = 8.5Hz, 2H), 7.55 (d, J = 8.5Hz, 2H), 7.83 (s, 1H), 7.97 (d, J = 7Hz, 1H), 10.09 (s, 1H), 10.16 (s, 1H), 12.03 (s, 1H). ^{13}C NMR (125 MHz, DMSO-d_6) δ (ppm): 22.64, 23.47, 26.15, 31.65, 43.69, 69.56, 87.47, 102.57, 107.37, 121.34, 123.83, 124.10, 126.43, 128.25, 132.00, 137.43, 138.51, 140.33, 148.84, 156.51, 156.71, 159.13, 159.70, 167.22. mp = 222.6–223.2 °C. HRMS (ESI) for $C_{25}H_{27}FN_3O_6$ $[M+H]^+$: Calcd, 484.1878; Found, 484.1884.

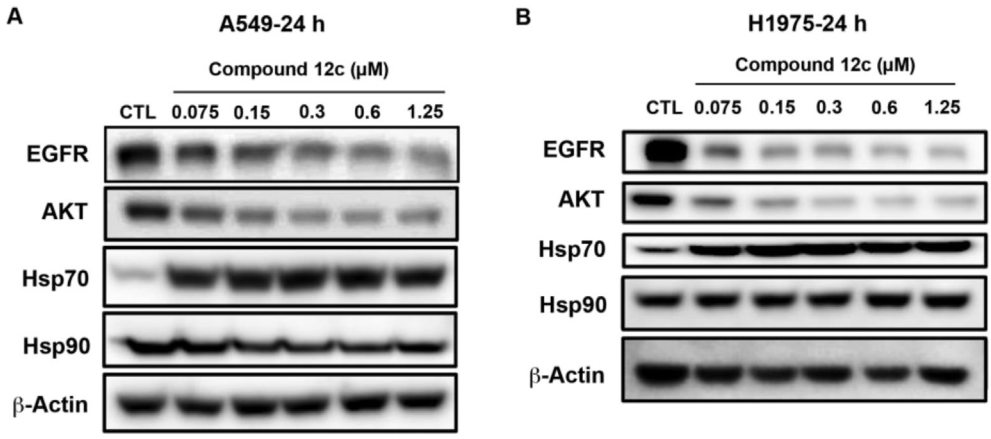

Fig. 5. Compound **12c** reduces HSP90 client proteins. (A–B) Compound **12c** suppresses protein expression level of HSP90 client proteins in NSCLC A549 (A) and H1975 (B) cells. Cells were treated with indicated concentrations for 24 h, and cell lysates were immunoblotted using the indicated antibodies.

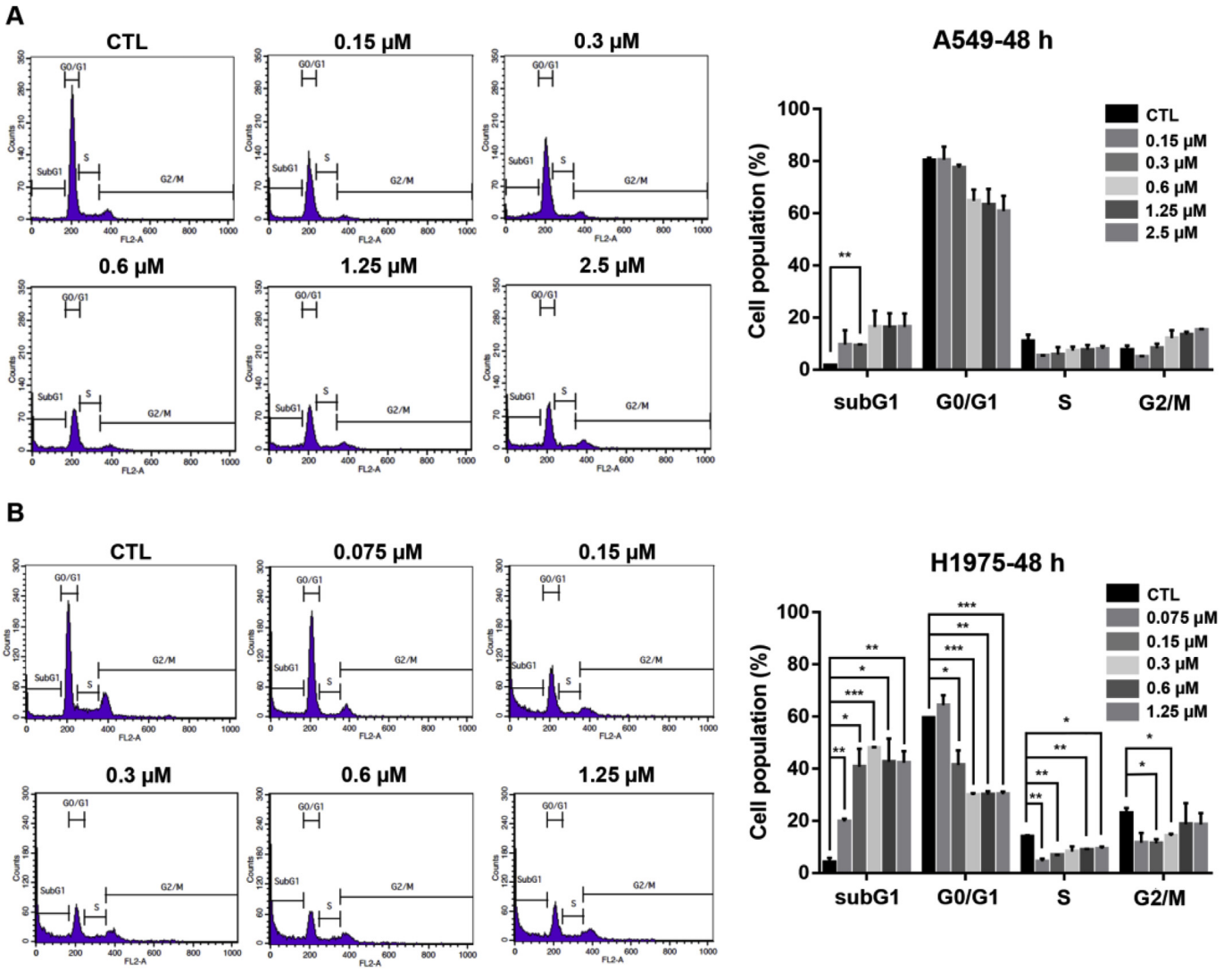

Fig. 6. Compound **12c** induces subG1 phase accumulation in NSCLC cells. (A–B) Concentration-dependent effects of Compound **12c** on subG1 phase accumulation in A549 (A) and H1975 (B) cells. Cells were treated with DMSO or Compound **12c** with indicated concentrations for the indicated times, and the cell cycle distribution was analyzed by flow cytometry. The right panel are quantitative data based on flow cytometry histograms, and are presented as means ± S.D. of at least three independent experiments that yielded similar results.

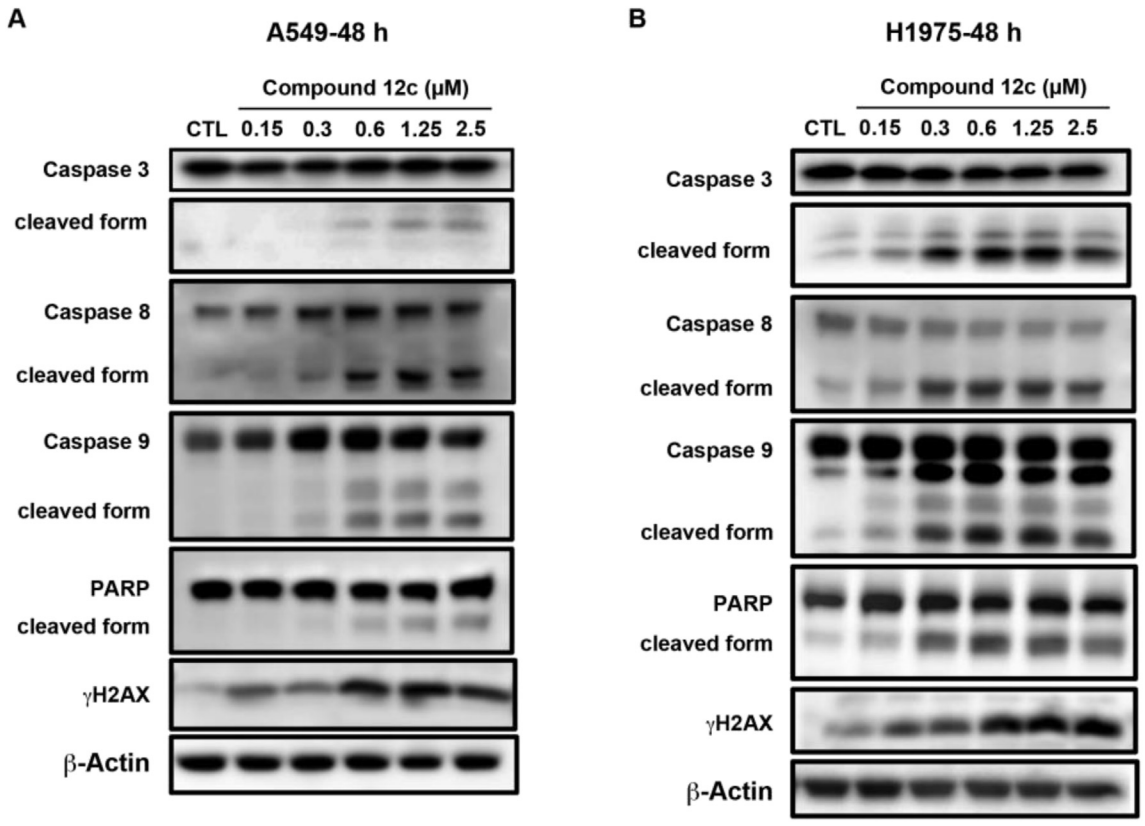

Fig. 7. Compound **12c** induces apoptosis in NSCLC. (A–B) Effects of compound **12c** on apoptosis in NSCLC cells. compound **12c** increased levels of the cleaved (activated) forms of PARP, γH2AX, caspase-3, -8, and -9 in a concentration-dependent manner. Cells were exposed to compound **12c** with indicated concentrations for 48 h, and cell lysates were immunoblotted using the indicated antibodies.

*4.1.2. N-(4-((5-Fluoro-2,6-dioxo-3-(tetrahydrofuran-2-yl)-3,6-dihydropyrimidin-1(2H)-yl)methyl)phenyl)-2,4-dihydroxy-5-isopropyl-N-methylbenzamide **(12b)***

A mixture of **16** (2.10mmole), NaH (2.52mmole), MeI (2.52mmole) and DMF (3 ml) was stirred at rt for 2 h. The reaction was quenched with water and extracted by EtOAc. The residue was purified by flash chromatography over silica gel to afford an intermediate. Then a mixture of this intermediate, 10% palladium on carbon (0.4 g) in MeOH (40 ml) was stirred at rt under hydrogen overnight. The organic layer was filtered and the residue was purified by flash chromatography over silica gel to afford compound **12b** in 42% yield. ^{1}H NMR (500 MHz, DMSO-d_6) δ (ppm): 0.63 (d, J = 3Hz, 3H), 0.65 (d, J = 3Hz, 3H), 1.89–1.96 (m, 2H), 1.97–2.01 (m, 1H), 2.20–2.26 (m, 1H), 2.75–2.80 (m, 1H), 3.29 (s, 3H), 3.80 (q, J = 7.5Hz, 1H), 4.24 (q, J = 6Hz, 1H), 4.91 (q, J = 14.5Hz, 2H), 5.92–5.94 (m, 1H), 6.18 (s, 1H), 6.45 (s, 1H), 7.13 (d, J = 8.5Hz, 2H), 7.29 (d, J = 8Hz, 2H), 7.95 (d, J = 6.5Hz, 2H), 10.72 (s, 1H). ^{13}C NMR (125 MHz, DMSO-d_6) δ (ppm): 22.07, 23.45, 24.96, 31.67, 38.17, 43.49, 69.59, 87.45, 102.27, 109.06, 123.76, 124.03, 124.63, 126.50, 127.72, 129.22, 134.58, 138.54, 140.35, 144.56, 148.77, 156.37, 156.57, 157.55, 157.85, 170.29. mp = 199.3–199.9 °C. HRMS (ESI) for $C_{26}H_{29}FN_3O_6$ $[M+H]^+$: Calcd, 498.2035; Found, 498.2041.

*4.1.3. N-Ethyl-N-(4-((5-fluoro-2,6-dioxo-3-(tetrahydrofuran-2-yl)-3,6-dihydropyrimidin-1(2H)-yl)methyl)phenyl)-2,4-dihydroxy-5-isopropylbenzamide **(12c)***

The title compound was obtained as a solid in 33% yield from compound **16** in a manner similar to that described for the preparation of **12b**. ^{1}H NMR (500 MHz, DMSO-d_6) δ (ppm): 0.60 (d, J = 3.1Hz, 3H), 0.61 (d, J = 3Hz, 3H), 1.06 (t, J = 7Hz, 3H), 1.89–1.92 (m, 2H), 1.97–2.00 (m, 1H), 2.20–2.28 (m, 1H), 2.72–2.78 (m, 1H), 3.76–3.83 (m, 3H), 4.23–4.27 (m, 1H), 4.92 (q, J = 14.5Hz, 2H), 5.92–5.94 (m, 1H), 6.17 (s, 1H), 6.42 (s, 1H), 7.12 (d, J = 8Hz, 2H), 7.32 (d, J = 8.5Hz, 2H), 7.95 (d, J = 6.5Hz, 2H), 9.76 (s, 1H), 10.93 (s, 1H). ^{13}C NMR (125 MHz, DMSO-d_6) δ (ppm): 12.52, 22.02, 23.44, 24.91, 31.67, 43.49, 45.13, 69.58, 87.44, 102.25, 123.75, 124.01, 124.54, 127.43, 127.75, 129.36, 134.81, 138.54, 140.36, 142.81, 148.77, 156.35, 156.56, 157.63, 158.44, 169.98. mp = 173.4–174.6 °C. HRMS (ESI) for $C_{27}H_{31}FN_3O_6$ $[M+H]^+$: Calcd, 512.2191; Found, 512.2195.

*4.1.4. N-(4-((5-Fluoro-2,6-dioxo-3-(tetrahydrofuran-2-yl)-3,6-dihydropyrimidin-1(2H)-yl)methyl)phenyl)-2,4-dihydroxy-5-isopropyl-N-propylbenzamide **(12d)***

The title compound was obtained as a solid in 42% yield from compound **16** in a manner similar to that described for the preparation of **12b.** ^{1}H NMR (500 MHz, DMSO-d_6) δ (ppm): 0.60 (d, J = 3.4Hz, 3H), 0.62 (d, J = 3.4Hz, 3H), 0.82 (t, J = 7Hz, 3H), 1.46–1.50 (m, 2H), 1.89–1.92 (m, 2H), 1.99–2.00 (m, 1H), 2.22–2.26 (m, 1H), 2.49–2.77 (m, 1H), 3.71 (t, J = 7.5H, 2H), 3.80 (q, J = 7.5Hz, 1H), 4.23–4.25 (m, 1H), 4.91 (q, J = 14.5Hz, 1H), 5.92–5.94 (m, 1H), 6.17 (s, 1H), 6.41 (s, 1H), 7.12 (d, J = 8Hz, 2H), 7.30 (d, J = 8.5Hz, 2H), 7.95 (d, J = 6.5Hz, 2H), 10.82 (s, 1H). ^{13}C NMR (125 MHz, DMSO-d_6) δ (ppm): 11.13, 14.08, 20.29, 22.05, 23.46, 24.93, 31.69, 43.50, 51.50, 69.60, 87.46, 102.27, 108.94, 123.76, 124.03, 124.56, 127.30, 127.66, 129.30, 134.73, 138.55, 140.37, 143.00, 148.79, 156.37, 156.58, 157.56, 158.20, 170.11. mp = 102.6–103.5 °C. HRMS (ESI) for $C_{28}H_{33}FN_3O_6$ $[M+H]^+$: Calcd, 526.2348; Found, 526.2354.

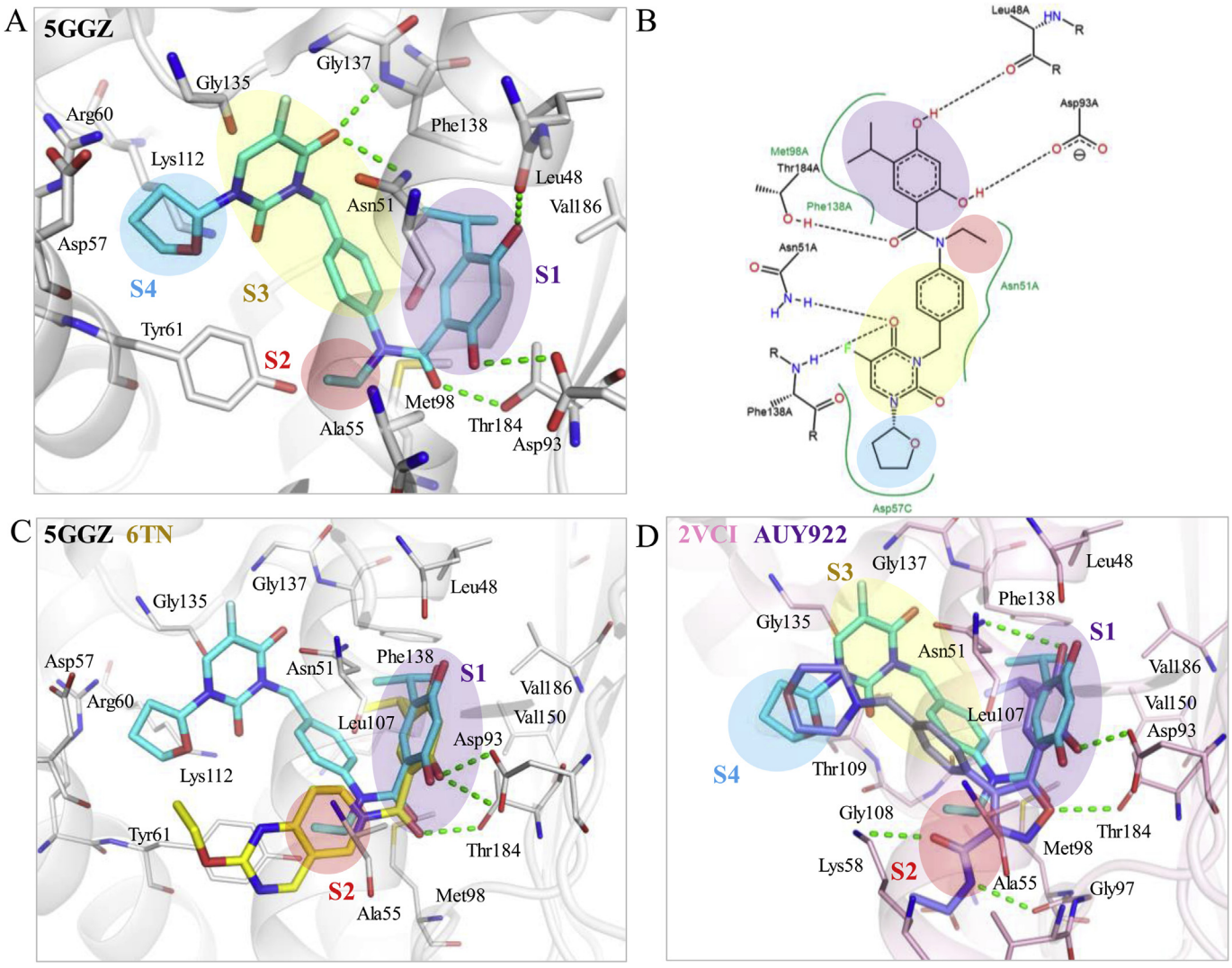

Fig. 8. Docking pose of compound **12c** in HSP90. (A) **12c** (blue) occupies the HSP90 (gray, PDB ID: 5GGZ) binding site. (B) A 2D representation of **12c** docked in HSP90. Hydrogen bonds are denoted by dashed lines, green lines represent areas of hydrophobic interactions. Interacting residues are labeled as shown. (C) The docking pose of **12c** superimposed with the co-crystal ligand, 6 TN. Overlapping sections are highlighted as previously described. (D) The docking pose of **12c** superimposed with the co-crystal ligand AUY-922 (purple, PDB ID: 2VCI). Interacting residues are labeled and represented as sticks. Hydrogen bonds are denoted by dotted green lines. The four distinct sites of **12c** are colored as purple, red, yellow and blue, which are located at sections S1, S2, S3 and S4, respectively. (For interpretation of the references to color in this figure legend, the reader is referred to the Web version of this article.)

*4.1.5. N-Benzyl-N-(4-((5-fluoro-2,6-dioxo-3-(tetrahydrofuran-2-yl)-3,6-dihydropyrimidin-1(2H)-yl)methyl)phenyl)-2,4-dihydroxy-5-isopropylbenzamide **(12e)***

The title compound was obtained as a solid in 32% yield from compound **16** in a manner similar to that described for the preparation of **12b.** ^{1}H NMR (500 MHz, DMSO-d_6) δ (ppm): 0.64 (d, J = 3Hz, 3H), 0.65 (d, J = 3.5Hz, 3H), 1.88–1.92 (m, 2H), 1.95–1.98 (m, 1H), 2.18–2.24 (m, 1H), 2.75–2.80 (m, 1H), 3.77–3.82 (m, 1H), 4.21–4.25 (m, 1H), 4.85 (q, J = 14Hz, 2H), 5.03 (s, 1H), 5.90–5.92 (m, 1H), 6.20 (s, 1H), 6.51 (s, 1H), 7.05 (d, J = 8.5Hz, 2H), 7.20–7.21 (m, 3H), 7.26–7.29 (m, 4H), 7.93 (d, J = 6.5Hz, 1H), 9.74 (s, 1H), 10.61 (s, 1H). ^{13}C NMR (125 MHz, DMSO-d_6) δ (ppm): 22.55, 23.91, 25.48, 32.15, 43.93, 53.44, 60.22, 70.05, 87.92, 102.78, 124.21, 124.48, 125.21, 127.45, 127.47, 128.10, 128.79, 129.44, 134.97, 137.93, 139.00, 140.81, 143.36, 149.22, 156.82, 157.02, 158.09, 158.18, 170.84. mp = 99.8–100.7 °C. HRMS (ESI) for $C_{32}H_{33}FN_3O_6$ $[M+H]^+$: Calcd, 574.2348; Found, 574.2353.

*4.1.6. N-(4-Cyanobenzyl)-N-(4-((5-fluoro-2,6-dioxo-3-(tetrahydrofuran-2-yl)-3,6-dihydropyrimidin-1(2H)-yl)methyl)phenyl)-2,4-dihydroxy-5-isopropylbenzamide **(12f)***

The title compound was obtained as a solid in 35% yield from compound **16** in a manner similar to that described for the preparation of **12b**. ^{1}H NMR (500 MHz, DMSO-d_6) δ (ppm): 0.67 (d, J = 3Hz, 3H), 0.68 (d, J = 3Hz, 3H), 1.88–1.92 (m, 2H), 1.97–1.98 (m, 2H), 2.18–2.24 (m, 1H), 2.76–2.80 (m, 1H), 3.77–3.82 (m, 1H), 4.21–4.25 (m, 1H), 4.86 (q, J = 14.5Hz, 2H), 5.11 (s, 1H), 5.90–5.91 (m, 1H), 6.19 (s, 1H), 6.55 (s, 1H), 7.09 (d, J = 8.5Hz, 2H), 7.20 (d, J = 8.5Hz, 2H), 7.49 (d, J = 8Hz, 2H), 7.75 (d, J = 8.5Hz, 2H), 7.93 (d, J = 7Hz, 1H), 9.74 (s, 1H), 10.45 (s, 1H). ^{13}C NMR (125 MHz, DMSO-d_6) δ (ppm): 22.09, 23.42, 25.04, 31.65, 43.43, 52.79, 69.57, 87.43, 102.28, 109.81, 118.75, 123.74, 124.01, 124.83, 126.85, 127.56, 128.43, 128.92, 132.29, 134.61, 138.50, 140.32, 142.66, 143.47, 148.74, 156.34, 156.54, 157.27, 157.59, 170.38. mp = 117.5–118.4 °C. HRMS (ESI) for $C_{33}H_{32}FN_4O_6$ $[M+H]^+$: Calcd, 599.2300; Found, 599.2307.

4.1.7. N-(4-Chlorobenzyl)-N-(4-((5-fluoro-2,6-dioxo-3-(tetrahydrofuran-2-yl)-3,6-dihydropyrimidin-1(2H)-yl)methyl) phenyl)-2,4-dihydroxy-5-isopropylbenzamide (12g)

The title compound was obtained as a solid in 34% yield from compound **16** in a manner similar to that described for the preparation of **12b** ^{1}H NMR (500 MHz, DMSO-d_6) δ (ppm): 0.64 (t, J = 2.1Hz, 6H), 1.89−1.94 (m, 2H), 1.95−1.97 (m, 1H), 2.20−2.24 (m, 1H), 3.79 (q, J = 7.5Hz, 1H), 4.83 (d, J = 14.5Hz, 1H), 4.88 (d, J = 14.5Hz, 1H), 5.01−5.03 (m, 2H), 5.89−5.92 (m, 1H), 6.20 (s, 1H), 6.50 (s, 1H), 7.05 (d, J = 8Hz, 2H), 7.19−7.21 (m, 3H), 7.26−7.33 (m, 4H), 7.92 (d, J = 6.5Hz, 1H). ^{13}C NMR (125 MHz, DMSO-d_6) δ (ppm): 22.20, 23.48, 25.06, 31.74, 43.52, 53.05, 69.65, 87.51, 102.37, 123.63, 124.80, 127.05, 127.08, 127.68, 128.38, 129.03, 129.69, 131.39, 134.33, 136.33, 137.15, 138.56, 140.13, 143.21, 148.81, 156.11, 157.84, 170.44. mp = 99.8−101.1C. HRMS (ESI) for $C_{32}H_{32}ClFN_3O_6$ $[M+H]^+$: Calcd, 608.1958; Found, 608.1962.

4.1.8. N-(4-((5-Fluoro-2,6-dioxo-3-(tetrahydrofuran-2-yl)-3,6-dihydropyrimidin-1(2H)-yl)methyl)phenyl)-2,4-dihydroxy-5-isopropyl-N-(4-methoxybenzyl)benzamide (12h)

The title compound was obtained as a solid in 35% yield from compound **16** in a manner similar to that described for the preparation of **12b**. ^{1}H NMR (500 MHz, DMSO-d_6) δ (ppm): 0.61 (d, J = 3.3Hz, 3H), 0.63 (d, J = 3.3Hz, 3H), 1.89−1.94 (m, 3H), 2,.20−2.24 (m, 1H), 2.74−2.77 (m, 1H), 3.77 (s, 3H), 4.21−4.25 (m, 1H), 4.86 (q, J = 14.5, 2H), 4.95 (s, 2H), 5.90−5.91 (m, 1H), 6.19 (s, 1H), 6.47 (s, 1H), 6.81 (d, J = 8.5Hz, 2H), 7.01 (d, J = 8Hz, 2H), 7.16 (d, J = 8.5Hz, 2H), 7.20 (d, J = 8.5Hz, 2H), 7.92 (d, J = 6.2Hz, 2H), 9.78 (s, 1H), 10.70 (s, 1H). ^{13}C NMR (125 MHz, DMSO-d_6) δ (ppm): 22.09, 23.4, 25.02, 31.72, 43.52, 55.00, 59.81, 69.64, 87.50, 102.34, 113.74, 123.77, 124.04, 124.75, 127.15, 127.72, 128.31, 129.06, 129.21, 129.29, 134.55, 138.56, 142.84, 148.80, 157.63, 158.35, 170.37. mp = 102.1−102.8 °C. HRMS (ESI) for $C_{33}H_{35}FN_3O_7$ [M+H]+: Calcd, 604.2454; Found, 604.2466.

4.1.9. N-Ethyl-N-(4-((5-fluoro-2,6-dioxo-3,6-dihydropyrimidin-1(2H)-yl)methyl)phenyl)-2,4-dihydroxy-5-isopropylbenzamide (13a)

A mixture of **16** (1.85 mmol), NaH (2.22 mmol), MeI (2.22 mmol) and DMF (3 ml) was stirred at 0 °C for 10 min and left at rt for 2 h. The reaction was quenched with water and extracted with EtOAc. The residue was purified by flash chromatography over silica gel to afford an intermediate compound. Then a mixture of the intermediate compound and boron trichloride (1 M) (17% in hexane) in CH_2Cl_2 was stirred at 0 °C for 3 h. The reaction was quenched with water and extracted with CH_2Cl_2. The organic layer was collected and dried over anhydrous $MgSO_4$ and concentrated *in vacuo* to yield an oily residue which was purified by flash chromatography over silica gel to afford compound **13a** in 36% yield. ^{1}H NMR (500 MHz, DMSO-d_6) δ (ppm): 0.34 (d, J = 7Hz, 6H), 0.78 (t, J = 6.5 Hz, 3H), 3.51 (q, J = 7Hz, 2H), 4.62 (s, 2H), 5.92 (s, 1H), 6.16 (s, 1H), 6.84 (d, J = 8.5Hz, 2H), 7.04 (d, J = 8Hz, 2H), 7.58 (t, J = 5.5Hz, 1H), 9.53 (s, 1H), 10.70 (s, 1H), 10.91 (d, J = 6Hz, 1H). ^{13}C NMR (125 MHz, DMSO-d_6) δ (ppm): 12.94, 22.52, 25.41, 43.35, 45.65, 102.73, 109.05, 125.06, 125.49, 125.74, 127.89, 128.28, 129.79, 135.56, 139.04, 140.84, 143.23, 150.28, 157.59, 157.80, 158.13, 159.01, 170.81. mp = 114.6−115.4 °C. HRMS (ESI) for $C_{23}H_{25}FN_3O_5$ $[M+H]^+$: Calcd, 442.1773; Found, 442.1780.

4.1.10. N-Allyl-N-(4-((5-fluoro-2,6-dioxo-3,6-dihydropyrimidin-1(2H)-yl)methyl)phenyl)-2,4-dihydroxy-5-isopropylbenzamide (13b)

The title compound was obtained as a solid in 42% yield from compound **16** in a manner similar to that described for the preparation of **13a**. ^{1}H NMR (300 MHz, DMSO-d_6) δ (ppm): 0.35 (d, J = 6.6Hz, 6H), 3.70 (q, J = 7.2Hz, 2H), 4.08 (d, J = 5.1Hz, 2H), 4.58 (s, 2H), 4.76−4.85 (m, 2H), 5.49−5.62 (m, 1H), 5.89 (s, 1H), 6.18 (s, 1H), 6.79 (d, J = 8.1Hz, 2H), 6.96 (d, J = 8.1Hz, 2H), 7.54 (t, J = 5.7Hz, 1H), 9.47 (s, 1H), 10.41 (s, 1H). ^{13}C NMR (125 MHz, DMSO-d_6) δ (ppm): 22.56, 25.46, 43.35, 53.09, 60.23, 102.74, 109.49, 117.84, 125.18, 125.52, 125.77, 127.54, 128.17, 129.48, 133.97, 135.34, 139.02, 140.83, 143.44, 150.28, 157.60, 157.80, 158.09, 158.42, 170.51. mp = 210.3−211.2 °C. HRMS (ESI) for $C_{24}H_{25}FN_3O_5$ $[M+H]^+$: Calcd, 454.1773; Found, 454.1778.

4.1.11. N-(4-((5-Fluoro-2,6-dioxo-3,6-dihydropyrimidin-1(2H)-yl) methyl)phenyl)-2,4-dihydroxy-5-isopropyl-N-(prop-2-yn-1-yl) benzamide (13c)

The title compound was obtained as a solid in 47% yield from compound **16** in a manner similar to that described for the preparation of **13a**. ^{1}H NMR (300 MHz, DMSO-d_6) δ (ppm): 0.67 (d, J = 3.9 Hz, 6H), 2.62−2.81 (m, 1H), 3.12 (s, 1H), 4.55 (d, J = 1.2Hz, 2H), 4.89 (s, 2H), 6.19 (s, 1H), 6.49 (s, 1H), 7.14 (d, J = 4.8Hz, 2H), 7.28 (d, J = 5.1Hz 2H), 7.84 (d, J = 3.3Hz 1H), 10.52 (s, 1H). ^{13}C NMR (125 MHz, DMSO-d_6) δ (ppm): 22.60, 25.48, 43.39, 75.05, 80.15, 102.78, 109.32, 125.60, 125.86, 127.71, 128.14, 129.42, 135.86, 139.02, 140.82, 142.71, 150.30, 157.61, 157.81, 158.21, 158.25, 170.35 mp = 214.2−214.9 °C. HRMS (ESI) for $C_{24}H_{23}FN_3O_5$ $[M+H]^+$: Calcd, 452.1616; Found, 452.1622.

4.1.12. 5-Fluoro-3-(4-nitrobenzyl)-1-(tetrahydrofuran-2-yl) pyrimidine-2,4(1H,3H)-dione (14)

A solution of 5-fluoro-1-(tetrahydrofuran-2-yl)pyrimidine-2,4(1H,3H)-dione (5.00 mmol), 1-(bromomethyl)-4-nitrobenzene (6.50 mmol), K_2CO_3 (6.50 mmol) in DMF (10 ml) was stirred at rt overnight. The reaction was quenched with water and extracted with EtOAc. The residue was purified by flash chromatography over silica gel to afford compound **15** in 70% yield. ^{1}H NMR (300 MHz, $CDCl_3$) δ (ppm): 1.95 (m, 1H), 2.06 (m, 2H), 2.40 (m, 1H), 3.97 (q, J = 2.1 Hz, 1H), 4.22 (m, 1H), 5.18 (q, J = 7.2 Hz, 2H), 5.97 (m, 1H), 7.42 (d, J = 5.7 Hz, 1H), 7.62 (d, J = 8.7Hz, 2H), 8.16 (d, J = 8.7 Hz, 2H).

4.1.13. 3-(4-Aminobenzyl)-5-fluoro-1-(tetrahydrofuran-2-yl) pyrimidine-2,4(1H,3H)-dione (15)

A mixture of **14** (0.69 mmol), iron powder (2.07 mmol), ammonium chloride (1.38 mmol), water (1.4 ml) and isopropyl alcohol (5.6 ml) was stirred reflux for 3 h. The reaction was quenched with water and extracted with EtOAc. The residue was purified by flash chromatography over silica gel to afford **15** in 81% yield. ^{1}H NMR (300 MHz $CDCl_3$) δ (ppm): 1.98 (m, 1H), 2.02 (m, 2H), 2.38 (m, 1H), 3.96, (q, J = 6.6 Hz, 1H), 4.20 (m, 1H), 5.03 (q, J = 4.2 Hz, 2H), 5.95 (m, 1H), 6.94 (d, J = 8.4 Hz, 2H), 7.35 (d, J = 5.7 Hz, 1H), 7.41 (d, J = 8.4 Hz, 2H).

4.1.14. 2,4-bis(Benzyloxy)-N-(4-((5-fluoro-2,6-dioxo-3-(tetrahydrofuran-2-yl)-3,6-dihydropyrimidin-1(2H)-yl)methyl) phenyl)-5-isopropylbenzamide (16)

A mixture of 2,4-bis(benzyloxy)-5-isopropylbenzoic acid (0.90 mmol), 1-ethyl-3-(3-dimethylaminopropyl)carbodiimide (1.13 mmol), hydroxybenzotriazole (0.90 mmol), N-methylmorpholine (1.13 mmol) and **15** (0.75 mmol) was stirred at rt overnight. The reaction was quenched with water and extracted with EtOAc. The residue was purified by flash chromatography over silica gel to afford compound **16** in 90% yield. ^{1}H NMR (300 MHz, $CDCl_3$): 1.25 (m, 6H), 1.93 (m, 1H), 2.02 (m, 1H), 2.05 (m, 1H), 2.38 (m, 1H), 3.34 (t, J = 6.9 Hz, 1H), 3.95 (q, J = 3.0Hz, 1H), 4.18 (m, 1H), 5.09−5.29 (m, 6H), 5,96 (m, 1H), 6.61 (m, 1H), 7.16−7.63 (m, 15H), 8.18 (s, 1H), 9.85 (s, 1H).

4.2. Biological activity

4.2.1. Cell lines and reagents

A549, H1975, and HCT116 cells were obtained from the American Type Culture Collection (ATCC) (Manassas, VA, USA). Cells were maintained in 10% fetal bovine serum (FBS)-supplemented RPMI 1640 medium (GIBCO, Grand Island, NY, USA) and 1% penicillin–streptomycin (GIBCO) at 37 °C in a humidified incubator containing 5% CO_2. Antibodies against various proteins were obtained from the following sources: PARP (Poly-ADP-ribose polymerase) was obtained from Santa Cruz Biotechnology Inc. (Dallas, TX, USA). Caspase 8, caspase 9, and γH2AX, were obtained from Cell signaling (Danvers, MA, USA). β-actin and GAPDH were obtained from Millipore (Billerica, MA, USA). Caspase 3 was obtained from Novous (Littleton, CO, USA). Anti-mouse and anti-rabbit IgGs were from Jackson ImmunoResearch Laboratories (West Grove, PA, USA).

4.2.2. HSP90 enzymatic assay

HSP90α Assay Kits (BPS Bioscience, San Diego, CA, USA) were utilized following the instruction manual, master mixture. HSP90 assay buffer, DTT, BSA, H_2O and FITC-labeled geldanamycin were added to all 96 wells. Then test compounds were added to each well designated "Test Inhibitor". To the "Blank", "Enzyme Positive Control" and "Enzyme Negative Control" wells, the same solution with inhibitor was added. HSP90 assay buffer was added to the "Enzyme Negative Control" and "Blank" wells. Finally, the recombinant protein HSP90α was incubated in every well designated "Enzyme Positive Control" and "Test Inhibitor" for 2–3 h at rt with slow shaking. The fluorescent polarization of the samples was determined by microtiter-plate reader, which can detect excitation ranging from 475 to 495 nm and emission ranging from 518 to 538 nm.

4.2.3. SRB (sulforhodamine B) assay

Cells were seeded in 96-well plates and cultured overnight followed by the exposure to gradient concentrations of different compounds for 48 h. Briefly, cells in Tz group were fixed *in situ* with 10% trichloroacetic acid (TCA) to represent a measurement of the cell population at the time of drug addition (T_0). After an additional 48 h incubation with or without compounds in medium with 5% FBS, the assay was terminated by 10% TCA in CTL and treatment groups. SRB dye purchased from Sigma (St. Louis, MO, USA) at 0.4% (w/v) in 1% acetic acid was added to stain the cells. Unbound dye was removed by 1% acetic acid and the plates were air dried. Bound dye was subsequently solubilized with 10 mM trizma base, and the absorbance was read at a wavelength of 515 nm.

4.2.4. Colony formation assay

Cells were plated in 96 well plates (5×10^3/well) and exposed to DMSO or compound **12c** at indicated concentrations for 24 h. The drugs were then washed away and cells were trypsinized and seeded in 24-well plates for continuing growth for 10 days. The colonies were fixed and stained with crystal violet (0.5% in 70% EtOH) and the experiments were repeated at least twice.

4.2.5. FACScan Flow Cytometric analysis

Cells were seeded in 6-well plates (2.5×10^5/well) and treated with DMSO or **12c** at various concentrations for indicated times. Cells were washed with phosphate-buffered saline, fixed in ice-cold 70% EtOH at −20 °C overnight, and stained with propidium iodide (80 μg/ml) containing Triton X-100 (0.1%, v/v) and RNase A (100 μg/ml) in phosphate-buffered saline (PBS). DNA content was analyzed with the FACScan and CellQuest software (Becton Dickinson, Mountain View, CA, USA).

4.2.6. Immunoblotting and lentivirus expression system

Cells were seeded in dishes and allowed to attach overnight. The cells were treated with drugs at indicated concentrations for indicated times. After the indicated exposure time, cells were lysed and the immunoblotting was performed as previously described [24].

4.2.7. Statistics and data analysis

Each experiment was performed at least three times, and representative data are shown. Data in bar graphs are given as the means ± S.D. Means were checked for statistical difference using the *t*-test and *P*-values less than 0.05 were considered significant ($*P < 0.05$, $**P < 0.01$, $***P < 0.001$).

4.3. Molecular docking study

The crystal structure of HSP90 (PDB ID: 5GGZ) was obtained from Protein Data Bank [25]. Protein preparation included removal of water molecules from the crystal structure. Docking was performed using the Knime [26] software and the FlexX node (https://www.biosolveit.de/knime/). The co-crystal structure was used to define the binding site. The 3D coordinates of docked compounds were generated using the "Generate 3D Coordinate" mode. Finally, all scoring parameters were used with the default settings.

Declaration of competing interest

The authors declare that they have no known competing financial interests or personal relationships that could have appeared to influence the work reported in this paper.

Acknowledgement

This work was financially supported by the Ministry of Science and Technology (MOST), Taiwan (Grant No. MOST 108-2320-B-038-056, 108-2320-B-038-064, MOST108-2320-B-038-027-MY3 and 108-2113-*M*-038-005) and the "TMU Research Center of Cancer Translational Medicine" from The Featured Areas Research Center Program within the framework of the Higher Education Sprout Project by the Ministry of Education (MOE) in Taiwan.

Appendix A. Supplementary data

Supplementary data to this article can be found online at https://doi.org/10.1016/j.ejmech.2020.112540.

References

[1] H. Wang, M. Lu, M. Yao, W. Zhu, Effects of treatment with an Hsp90 inhibitor in tumors based on 15 phase II clinical trials, Mol Clin Oncol 5 (3) (2016 Sep) 326–334.

[2] (a) S.C. Gupta, A. Sharma, M. Mishra, R.K. Mishra, D.K. Chowdhuri, Heat shock proteins in toxicology: how close and how far? Life Sci. 86 (11-12) (2010 Mar 13) 377–384;
(b) C.J. Park, Y.S. Seo, Heat shock proteins: a review of the molecular chaperones for plant immunity, Plant Pathol. J. 31 (4) (2015 Dec) 323–333.

[3] (a) A. Hoter, M.E. El-Sabban, H.Y. Naim, The HSP90 family: structure, regulation, function, and implications in health and disease, Int. J. Mol. Sci. 19 (9) (2018 Aug 29) E2560, pii;
(b) O. Genest, S. Wickner, S.M. Doyle, Hsp90 and Hsp70 chaperones: collaborators in protein remodeling, J. Biol. Chem. 294 (6) (2019 Feb 8) 2109–2120;
(c) F.H. Schopf, M.M. Biebl, J. Buchner, The HSP90 chaperone machinery, Nat. Rev. Mol. Cell Biol. 18 (6) (2017 Jun) 345–360.

[4] (a) W. Luo, W. Sun, T. Taldone, A. Rodina, G. Chiosis, Heat shock protein 90 in neurodegenerative diseases, Mol. Neurodegener. 5 (2010 Jun 3) 24;
(b) J.J. Barrott, T.A. Haystead, Hsp90, an unlikely ally in the war on cancer, FEBS J. 280 (6) (2013 Mar) 1381–1396;
(c) N. Roy, R.K. Nageshan, S. Ranade, U. Tatu, Heat shock protein 90 from neglected protozoan parasites, Biochim. Biophys. Acta 1823 (3) (2012 Mar) 707–711;
(d) R. Geller, S. Taguwa, J. Frydman, Broad action of Hsp90 as a host chaperone

required for viral replication, Biochim. Biophys. Acta 1823 (3) (2012 Mar) 698–706;
(e) H. Fuhrmann-Stroissnigg, Y.Y. Ling, J. Zhao, S.J. McGowan, Y. Zhu, R.W. Brooks, D. Grassi, S.Q. Gregg, J.L. Stripay, A. Dorronsoro, L. Corbo, P. Tang, C. Bukata, N. Ring, M. Giacca, X. Li, T. Tchkonia, J.L. Kirkland, L.J. Niedernhofer, P.D. Robbins, Identification of HSP90 inhibitors as a novel class of senolytics, Nat. Commun. 8 (1) (2017 Sep 4) 422.

[5] (a) E. Vartholomaiou, P.C. Echeverría, D. Picard, Unusual suspects in the twilight zone between the Hsp90 interactome and carcinogenesis, Adv. Canc. Res. 129 (2016) 1–30;
(b) P.J. Webber, C. Park, M. Qui, S.S. Ramalingam, F.R. Khuri, H. Fu, Y. Du, Combination of heat shock protein 90 and focal adhesion kinase inhibitors synergistically inhibits the growth of non-small cell lung cancer cells, Oncoscience 2 (9) (2015 Sep 15) 765–776;
(c) Y.V. Liu, J.H. Baek, H. Zhang, R. Diez, R.N. Cole, G.L. Semenza, RACK1 competes with HSP90 for binding to HIF-1alpha and is required for O(2)-independent and HSP90 inhibitor-induced degradation of HIF-1alpha, Mol. Cell. 25 (2) (2007 Jan 26) 207–217.

[6] E. Pick, Y. Kluger, J.M. Giltnane, C. Moeder, R.L. Camp, D.L. Rimm, H.M. Kluger, High HSP90 expression is associated with decreased survival in breast cancer, Canc. Res. 67 (7) (2007 Apr 1) 2932–2937.

[7] K. Jhaveri, S.O. Ochiana, M.P. Dunphy, J.F. Gerecitano, A.D. Corben, R.I. Peter, Y.Y. Janjigian, E.M. Gomes-DaGama, J. Koren 3rd, S. Modi, G. Chiosis, Heat shock protein 90 inhibitors in the treatment of cancer: current status and future directions, Expet Opin. Invest. Drugs 23 (5) (2014 May) 611–628.

[8] R.N. Pillai, S.S. Ramalingam, Heat shock protein 90 inhibitors in non-small-cell lung cancer, Curr. Opin. Oncol. 26 (2) (2014 Mar) 159–164.

[9] D.B. Longley, D.P. Harkin, P.G. Johnston, 5-fluorouracil: mechanisms of action and clinical strategies, Nat. Rev. Canc. 3 (5) (2003 May) 330–338.

[10] (a) C. Bailly, Irinotecan: 25 years of cancer treatment, Pharmacol. Res. 148 (2019 Oct) 104398;
(b) J. Giuliani, A. Bonetti, First-line therapies in metastatic colorectal cancer: integrating clinical benefit with the costs of drugs, Int. J. Colorectal Dis. 33 (11) (2018 Nov) 1505–1516.

[11] B.R. Hirsch, S.Y. Zafar, Capecitabine in the management of colorectal cancer, Canc. Manag. Res. 3 (2011) 79–89.

[12] (a) V. Heinemann, L.F. von Weikersthal, T. Decker, A. Kiani, U. Vehling-Kaiser, S.E. Al-Batran, T. Heintges, C. Lerchenmüller, C. Kahl, G. Seipelt, F. Kullmann, M. Stauch, W. Scheithauer, J. Hielscher, M. Scholz, S. Müller, H. Link, N. Niederle, A. Rost, H.G. Höffkes, M. Moehler, R.U. Lindig, D.P. Modest, L. Rossius, T. Kirchner, A. Jung, S. Stintzing, FOLFIRI plus cetuximab versus FOLFIRI plus bevacizumab as first-line treatment for patients with metastatic colorectal cancer (FIRE-3): a randomised, open-label, phase 3 trial, Lancet Oncol. 15 (10) (2014 Sep) 1065–1075;
(b) C. Cremolini, F. Loupakis, C. Antoniotti, C. Lupi, E. Sensi, S. Lonardi, S. Mezi, G. Tomasello, M. Ronzoni, A. Zaniboni, G. Tonini, C. Carlomagno, G. Allegrini, S. Chiara, M. D'Amico, C. Granetto, M. Cazzaniga, L. Boni, G. Fontanini, A. Falcone, FOLFOXIRI plus bevacizumab versus FOLFIRI plus bevacizumab as first-line treatment of patients with metastatic colorectal cancer: updated overall survival and molecular subgroup analyses of the open-label, phase 3 TRIBE study, Lancet Oncol. 16 (13) (2015 Oct) 1306–1315;
(c) S. Stintzing, D.P. Modest, L. Rossius, M.M. Lerch, L.F. von Weikersthal, T. Decker, A. Kiani, U. Vehling-Kaiser, S.E. Al-Batran, T. Heintges, C. Lerchenmüller, C. Kahl, G. Seipelt, F. Kullmann, M. Stauch, W. Scheithauer, S. Held, C. Giessen-Jung, M. Moehler, A. Jagenburg, T. Kirchner, A. Jung, V. Heinemann, FIRE-3 investigators. FOLFIRI plus cetuximab versus FOLFIRI plus bevacizumab for metastatic colorectal cancer (FIRE-3): a post-hoc analysis of tumour dynamics in the final RAS wild-type subgroup of this randomised open-label phase 3 trial, Lancet Oncol. 17 (10) (2016 Oct) 1426–1434.

[13] (a) Y. Chihara, A. Yoshimura, K. Date, Y. Takemura, N. Tamiya, Y. Kohno, T. Imabayashi, M. Takeuchi, Y. Kaneko, T. Yamada, M. Ueda, T. Arimoto, J. Uchino, Y. Iwasaki, K. Takayama, Phase II study of S-1 and paclitaxel combination therapy in patients with previously treated non-small cell lung cancer, Oncol. 24 (8) (2019 Aug) 1033. -e617;
(b) Q. Lin, F.J. Meng, Y. Liu, N. Wang, X.C. Ren, X.J. Chen, X.H. Ge, C.X. Liu, Jing-Hu, D.Y. Wang, B. Cao, Y. Zhao, Phase II trial of capecitabine combined with docetaxel in previously treated patients with non-small cell lung cancer: a randomized controlled study, Oncol Lett 3 (4) (2012 Apr 1) 761–766.

[14] D.R. Camidge, W. Pao, L.V. Sequist, Acquired resistance to TKIs in solid tumours: learning from lung cancer, Nat. Rev. Clin. Oncol. 11 (8) (2014 Aug) 473–481.

[15] C. Ma, S. Wei, Y. Song, T790M and acquired resistance of EGFR TKI: a literature review of clinical reports, J. Thorac. Dis. 3 (1) (2011 Mar) 10–18.

[16] (a) M. Takeda, K. Nakagawa, First- and second-generation EGFR-TKIs are all replaced to osimertinib in chemo-naive EGFR mutation-positive non-small cell lung cancer? Int. J. Mol. Sci. 20 (1) (2019 Jan 3) E146, pii:;
(b) X. Wang, D. Goldstein, P.J. Crowe, J.L. Yang, Next-generation EGFR/HER tyrosine kinase inhibitors for the treatment of patients with non-small-cell lung cancer harboring EGFR mutations: a review of the evidence, OncoTargets Ther. 9 (2016 Sep 6) 5461–5473;
(c) M. Soda, Y.L. Choi, M. Enomoto, S. Takada, Y. Yamashita, S. Ishikawa, S. Fujiwara, H. Watanabe, K. Kurashina, H. Hatanaka, M. Bando, S. Ohno, Y. Ishikawa, H. Aburatani, T. Niki, Y. Sohara, Y. Sugiyama, H. Mano, Identification of the transforming EML4-ALK fusion gene in non-small-cell lung cancer, Nature 448 (7153) (2007 Aug 2) 561–566.

[17] (a) L.V. Sequist, B.A. Waltman, D. Dias-Santagata, S. Digumarthy, A.B. Turke, P. Fidias, K. Bergethon, A.T. Shaw, S. Gettinger, A.K. Cosper, S. Akhavanfard, R.S. Heist, J. Temel, J.G. Christensen, J.C. Wain, T.J. Lynch, K. Vernovsky, E.J. Mark, M. Lanuti, A.J. Iafrate, M. Mino-Kenudson, J.A. Engelman, Genotypic and histological evolution of lung cancers acquiring resistance to EGFR inhibitors, Sci. Transl. Med. 3 (75) (2011 Mar 23), 75ra26;
(b) K. Ohashi, Y.E. Maruvka, F. Michor, W. Pao, Epidermal growth factor receptor tyrosine kinase inhibitor-resistant disease, J. Clin. Oncol. 31 (8) (2013 Mar 10) 1070–1080;
(c) S. Yano, T. Yamada, S. Takeuchi, K. Tachibana, Y. Minami, Y. Yatabe, T. Mitsudomi, H. Tanaka, T. Kimura, S. Kudoh, H. Nokihara, Y. Ohe, J. Yokota, H. Uramoto, K. Yasumoto, K. Kiura, M. Higashiyama, M. Oda, H. Saito, J. Yoshida, K. Kondoh, M. Noguchi, Hepatocyte growth factor expression in EGFR mutant lung cancer with intrinsic and acquired resistance to tyrosine kinase inhibitors in a Japanese cohort, J. Thorac. Oncol. 6 (12) (2011 Dec) 2011–2017;
(d) S. Kobayashi, T.J. Boggon, T. Dayaram, P.A. Jänne, O. Kocher, M. Meyerson, B.E. Johnson, M.J. Eck, D.G. Tenen, B. Halmos, EGFR mutation and resistance of non-small-cell lung cancer to gefitinib, N. Engl. J. Med. 352 (8) (2005 Feb 24) 786–792.

[18] (a) T. Seto, T. Kato, M. Nishio, K. Goto, S. Atagi, Y. Hosomi, N. Yamamoto, T. Hida, M. Maemondo, K. Nakagawa, S. Nagase, I. Okamoto, T. Yamanaka, K. Tajima, R. Harada, M. Fukuoka, N. Yamamoto, Erlotinib alone or with bevacizumab as first-line therapy in patients with advanced non-squamous non-small-cell lung cancer harbouring EGFR mutations (JO25567): an open-label, randomised, multicentre, phase 2 study, Lancet Oncol. 15 (11) (2014 Oct) 1236–1244;
(b) M. Reck, E.B. Garon, L. Paz-Ares, S. Ponce, J.C. Jaime, O. Juan, E. Nadal, K. Kiura, R.C. Widau, S. He, R. Dalal, P. Lee, K. Nakagawa, Randomized, double-blind phase ib/III study of erlotinib with ramucirumab or placebo in previously untreated EGFR-mutant metastatic non-small-cell lung cancer (RELAY): phase ib results, Clin. Lung Canc. 19 (3) (2018 May) 213–220;
(c) P. Shi, Y.T. Oh, L. Deng, G. Zhang, G. Qian, S. Zhang, H. Ren, G. Wu, B. Legendre Jr., E. Anderson, S.S. Ramalingam, T.K. Owonikoko, M. Chen, S.Y. Sun, Overcoming acquired resistance to AZD9291, A third-generation EGFR inhibitor, through modulation of MEK/ERK-dependent bim and mcl-1 degradation, Clin. Canc. Res. 23 (21) (2017 Nov 1) 6567–6579;
(d) Z. Yang, K.Y. Tam, Combination strategies using EGFR-TKi in NSCLC therapy: learning from the gap between pre-clinical results and clinical outcomes, Int. J. Biol. Sci. 14 (2) (2018 Feb 5) 204–216.

[19] (a) J. Nakano, C. Huang, D. Liu, D. Masuya, T. Nakashima, H. Yokomise, M. Ueno, H. Wada, M. Fukushima, Evaluations of biomarkers associated with 5-FU sensitivity for non-small-cell lung cancer patients postoperatively treated with UFT, Br. J. Canc. 95 (5) (2006 Sep 4) 607–615;
(b) J.G. Zhao, K.M. Ren, J. Tang, Overcoming 5-Fu resistance in human non-small cell lung cancer cells by the combination of 5-Fu and cisplatin through the inhibition of glucose metabolism, Tumour Biol 35 (12) (2014 Dec) 12305–12315.

[20] (a) T. Shimamura, S.A. Perera, K.P. Foley, J. Sang, S.J. Rodig, T. Inoue, L. Chen, D. Li, J. Carretero, Y.C. Li, P. Sinha, C.D. Carey, C.L. Borgman, J.P. Jimenez, M. Meyerson, W. Ying, J. Barsoum, K.K. Wong, G.I. Shapiro, Ganetespib (STA-9090), a nongeldanamycin HSP90 inhibitor, has potent antitumor activity in in vitro and in vivo models of non-small cell lung cancer, Clin. Canc. Res. 18 (18) (2012 Sep 15) 4973–4985;
(b) E.B. Garon, R.S. Finn, H. Hamidi, J. Dering, S. Pitts, N. Kamranpour, A.J. Desai, W. Hosmer, S. Ide, E. Avsar, M.R. Jensen, C. Quadt, M. Liu, S.M. Dubinett, D.J. Slamon, The HSP90 inhibitor NVP-AUY922 potently inhibits non-small cell lung cancer growth, Mol. Canc. Therapeut. 12 (6) (2013 Jun) 890–900.

[21] H. Dimant, D. Ebrahimi-Fakhari, P.J. McLean, Molecular chaperones and co-chaperones in Parkinson disease, Neuroscientist 18 (6) (2012 Dec) 589–601.

[22] F. Jiang, H.J. Wang, Y.H. Jin, et al., Novel tetrahydropyrido[4,3-d]pyrimidines as potent inhibitors of chaperone heat shock protein 90, J. Med. Chem. 59 (23) (2016) 10498–10519.

[23] P.A. Brough, W. Aherne, X. Barril, et al., 4,5-diarylisoxazole Hsp90 chaperone inhibitors: potential therapeutic agents for the treatment of cancer, J. Med. Chem. 51 (2) (2008) 196–218.

[24] C.H. Chen, C.A. Changou, T.H. Hsieh, Y.C. Lee, C.Y. Chu, K.C. Hsu, H.C. Wang, Y.C. Lin, Y.N. Lo, Y.R. Liu, J.P. Liou, Y. Yen, Dual inhibition of PIK3C3 and FGFR as a new therapeutic approach to treat bladder cancer, Clin. Canc. Res. 24 (5) (2018 Mar 1) 1176–1189.

[25] H.M. Berman, et al., The protein Data Bank, Nucleic Acids Res. 28 (2000) 235–242.

[26] R. Michael, N.C. Berthold, Fabian Dill, Thomas R. Gabriel, Tobias Kötter, Thorsten meinl, peter ohl, christoph sieb, killian thiel, bernd wiswedel, in: Studies in Classification, Data Analysis, and Knowledge Organization (GfKL 2007), Springer, 2007.